Spin-Dependent Electron-Proton Scattering in the Δ-Excitation Region

L. D. van Buuren,[1,2] D. Szczerba,[3] R. Alarcon,[4] D. J. Boersma,[1] J. F. J. van den Brand,[1,2] H. J. Bulten,[1,2] R. Ent,[5,6] M. Ferro-Luzzi,[1,2] M. Harvey,[5,6] P. Heimberg,[1,2] D. W. Higinbotham,[1,7] S. Klous,[1,2] H. Kolster,[1,2] J. Lang,[3] B. L. Militsyn,[1] D. Nikolenko,[8] B. E. Norum,[7] I. Passchier,[1] H. R. Poolman,[1,2] I. Rachek,[8] M. C. Simani,[1,2] E. Six,[4] H. de Vries,[1] and Z.-L. Zhou[9]

[1]*National Institute for Nuclear Physics and High Energy Physics, NL-1009 DB Amsterdam, The Netherlands*
[2]*Department of Physics and Astronomy, Vrije Universiteit, NL-1081 HV, Amsterdam, The Netherlands*
[3] *Institut für Teilchenphysik, Eidgenössische Technische Hochschule, CH-8093 Zürich, Switzerland*
[4]*Department of Physics and Astronomy, Arizona State University, Tempe, Arizona 85287*
[5]*Department of Physics, Hampton University, Hampton, Virginia 23668*
[6]*TJNAF, Newport News, Virginia 23606*
[7]*Department of Physics, University of Virginia, Charlottesville, Virginia 22901*
[8]*Budker Institute for Nuclear Physics, Novosibirsk 630090, Russian Federation*
[9]*Laboratory for Nuclear Science, Massachusetts Institute of Technology, Cambridge, Massachusetts 02139*

(Received 19 February 2002; published 18 June 2002)

We report on measurements of the cross section and provide first data on spin correlation parameters $A_{TT'}$ and $A_{TL'}$ in inclusive scattering of longitudinally polarized electrons from nuclear-polarized hydrogen. Polarized electrons were injected into an electron storage ring operated at a beam energy of 720 MeV. Polarized hydrogen was produced by an atomic beam source and injected into an open-ended cylindrical cell, located in the electron storage ring. The four-momentum transfer squared ranged from $Q^2 = 0.2$ GeV$^2/c^2$ at the elastic scattering peak to $Q^2 = 0.11$ GeV$^2/c^2$ at the $\Delta(1232)$ resonance. The data provide a stringent test of pion electroproduction models.

DOI: 10.1103/PhysRevLett.89.012001 PACS numbers: 13.60.Le, 13.88.+e, 14.20.Gk, 25.30.Rw

The structure of the nucleon continues to be a topic of intense theoretical and experimental studies in subatomic physics. In particular, pion electro- [1] and photoproduction [2] data have been used to extract detailed information on the baryon spin structure. Electromagnetic pion production from the nucleon may be analyzed in terms of multipoles, usually denoted $T_{\ell\pm}$ (see, e.g., Refs. [3,4]), where $T = M$, E, or S describes the type of transition (magnetic, electric, or scalar), while ℓ and $J = \ell \pm 1/2$ indicate the orbital angular momentum and total spin of the πN system, respectively.

Experimentally, one finds that pion production in the Δ resonance region is dominated by the M_{1+} multipole. At four-momentum transfer $Q = 0$, polarized photon experiments have established the presence of a small but nonzero E_{1+} component [2]. Similarly, nonvanishing S_{1+} and E_{1+} amplitudes have been determined in several electron scattering experiments [1]. In order to reliably associate such information with subtle features of baryon structure, models are required that can accurately describe the reaction mechanism of $\gamma^* p \rightarrow \pi N$ and that are able to disentangle resonant from nonresonant contributions. A dispersion relation approach has been used to single out the importance of such nonresonant contributions, even in the so-called "resonant" multipoles $M_{1+}^{3/2}$, $E_{1+}^{3/2}$, and $S_{1+}^{3/2}$ [5] (here, the superscript specifies the isospin channel); dynamical model approaches tend to show large nonresonant contributions as well, due to pion rescattering [6,7]; the role of the pion cloud [8] or two-body exchange currents [9] in quark models has been stressed in several articles. Furthermore, it was shown in a nonrelativistic consistent quark model calculation that exchange currents alone can generate nonzero $E_{1+}^{3/2}$ and $S_{1+}^{3/2}$ amplitudes, without the need of a D-state admixture in the baryon wave function [10]. Ultimately, a model should be developed which consistently describes *both* baryon structure *and* the reaction mechanism.

Here, we present the results of the first experiment in which both longitudinal and transverse spin correlation parameters of the $^1\vec{\mathrm{H}}(\vec{e}, e')$ reaction have been measured in the $\Delta(1232)$ resonance region. The experiment covered a Q^2 range from 0.2 (elastic scattering peak) to about 0.08 GeV$^2/c^2$ (at $W \approx 1.3$ GeV, with W the invariant mass of the undetected particles). The spin-dependent differential cross section for inclusive scattering of longitudinally polarized electrons (beam energy E, polarization P_e) from a polarized proton target (mass M_p, polarization P_p oriented in the scattering plane) is given by (see, e.g., in Refs. [3,4])

$$\frac{d\sigma}{d\Omega_e dE'} = \frac{\alpha}{2\pi^2}\frac{E'}{E}\frac{W^2 - M_p^2}{2M_p Q^2}\frac{1}{1-\epsilon}\,\sigma(\nu, Q^2),$$
$$\frac{\sigma}{\sigma_0} = 1 + P_e P_p(\cos\theta^* A_{TT'} + \sin\theta^*\cos\phi^* A_{TL'}), \tag{1}$$

with α the fine-structure constant, E' the energy of the scattered electron, and $\nu = E - E'$ the transferred energy. The polar and azimuthal angles of the target polarization axis are denoted with θ^* and ϕ^* in the right-hand frame,

where the y axis is defined by the vector product of the incoming and outgoing electron momenta, $\mathbf{k} \times \mathbf{k}'$, and the z axis is along the three-momentum transfer $\mathbf{q} = \mathbf{k} - \mathbf{k}'$. Furthermore, $\epsilon^{-1} = 1 + (2\mathbf{q}^2/Q^2)\tan^2(\theta_e/2)$ with θ_e the electron scattering angle. The spin-averaged part of the cross section, $\sigma_0 \equiv \sigma_T + \epsilon\sigma_L$, contains the usual longitudinal (σ_L) and transverse (σ_T) terms. In our experiment, we determine the quantity $A \equiv (\sigma_+ - \sigma_-)/(\sigma_+ + \sigma_-)$, where $\sigma_\pm$ are given by Eq. (1) with $P_e P_p = \pm 1$. In the following, we call $A_{\|\mathbf{q}_\Delta}$ and $A_{\perp\mathbf{q}_\Delta}$ the observable A which we measured with the target polarization axis antiparallel ($\theta^* = \pi$) and perpendicular ($\theta^* = \pi/2, \phi^* = 0$) to the average direction of $\mathbf{q}$ for $W = 1232$ MeV. From these we can determine both $A_{TT'}$ and $A_{TL'}$.

Inclusive scattering measures the total virtual photon absorption probability. When compared with exclusive scattering experiments, the interest of this approach lies in the reduced sensitivity to final-state interaction and in the fact that different interference terms contribute to the cross section. For instance, in the inclusive ep reaction the M_{1+} multipole interferes only with the E_{1+} and S_{1+} multipoles (or with itself, as in $A_{TT'}$), in contrast to the case of exclusive reactions. Since in the Δ resonance region M_{1+} dominates, other multipole contributions are suppressed with respect to those of E_{1+} and S_{1+}.

The experiment was performed with a polarized gas target internal to the Amsterdam Pulse Stretcher (AmPS) storage ring, as shown in Fig. 1. An atomic beam source (ABS) [11] was used to inject a flux of 6×10^{16} atoms/s (in two hyperfine states) into the Ø12 mm feed tube of a cylindrical storage cell cooled to 70 K. The cell had a diameter of 15 mm and was 60 cm long, resulting in a typical target thickness of 10^{14} protons/cm^2. An electromagnet was used to provide a guide field of 0.04 T over the storage cell. The sign of the target polarization was varied every 8 s by switching on and off high-frequency transitions in the ABS. The injected atomic beam intensity and polarization were optimized and monitored by sampling a fraction of the atomic beam through a Ø4 mm hole in the storage cell into a Breit-Rabi-type polarimeter (BRP).

Polarized electrons, produced by photoemission from a strained-layer semiconductor cathode (InGaAsP), were accelerated to 720 MeV, and stacked in the AmPS storage ring. Beam currents of more than 100 mA with a lifetime in excess of 15 min were obtained. Every 5 min, the remaining electrons were dumped, and the ring was refilled after reversal of the electron polarization at the source. The polarization of the stored electrons was maintained using the "Siberian Snake" principle [12]. The electron beam polarization was checked and optimized at the source with a Mott polarimeter [13] and in the ring with a Compton backscattering polarimeter [14].

Scattered electrons were detected in the large-acceptance magnetic spectrometer Bigbite [15] positioned at a central scattering angle of 40°, with a momentum acceptance from 250 to 720 MeV/c and a solid angle

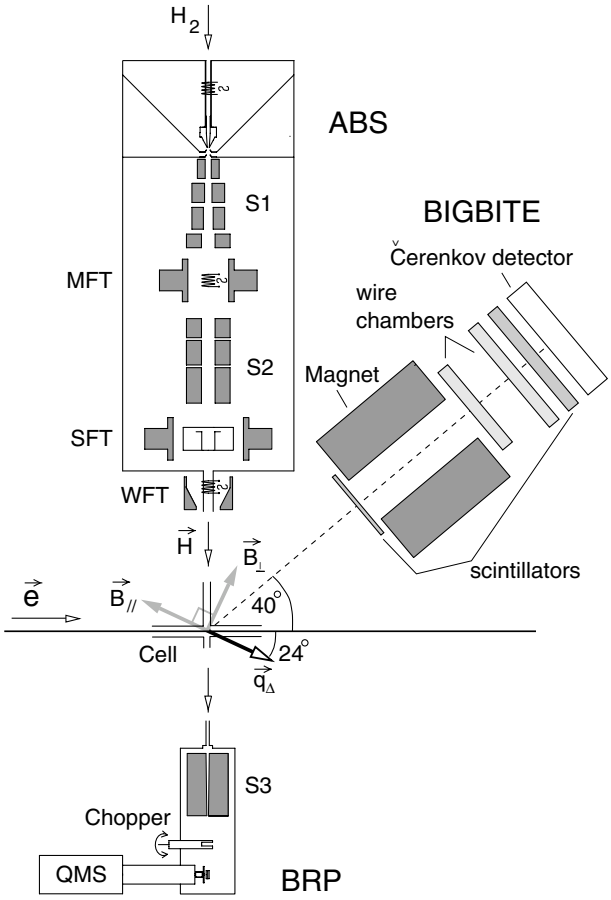

FIG. 1. Schematical layout of the experiment. The electron spectrometer (Bigbite [15]) consists of a 4 mm thick scintillator, a 1 Tm dipole magnet, two drift chambers of four planes each, a second scintillator, and a Čerenkov detector. The atomic beam source (ABS) and Breit-Rabi polarimeter (BRP) contain the components needed for producing and analyzing polarized hydrogen [11]. MFT, SFT, WFT: high-frequency transition units. S1, S2, and S3: Stern-Gerlach sextupole magnets. QMS: quadrupole mass spectrometer. The two target field orientations used are indicated by $\vec{B}_\|$ and $\vec{B}_\perp$. The average direction of the three-momentum transfer at $W = 1232$ MeV is depicted as $\vec{q}_\Delta$.

of 96 msr (see Fig. 1). This setting resulted in a central value of $Q^2 = 0.2$ GeV$^2/c^2$ for elastic scattering ($W = 938.3$ MeV) and $Q^2 = 0.11$ GeV$^2/c^2$ for the Δ resonance ($W = 1232$ MeV). The contribution of events due to electrons scattering from the cell has been taken into account by subtracting from the total rates the normalized rate of cell events, which we measured intermittently with an empty storage cell. The presence of target gas in the cell may change the background event rate, e.g., because of an emittance increase of the stored electron beam due to trapped ions. We monitored this by analyzing event rates in a kinematical region dominated by scattering from the cell walls. The cell event rate was found to be on average 1.73 ± 0.13 times higher when injecting hydrogen into the cell, and its contribution

amounted to 2.8% at the elastic scattering peak and 43% at the Δ resonance.

In this work, we compare our data to predictions from the models of Drechsel *et al.* [16] (MAID) and of Sato and Lee (SL) [7]. Both models start from an effective Lagrangian approach that includes light meson (π, ρ, and ω), nucleon (N and N^*), and photon fields. They both satisfy gauge invariance and differ mainly in the way of implementing unitarity and constraining model parameters from data. To compare these theoretical results to our data, while taking into account finite acceptance effects and small variations of the target field angle over the cell region, we developed a Monte Carlo (MC) code that interpolated the model predictions between a dense grid of calculations over the entire kinematical range and detector acceptance. Furthermore, we have taken into account radiative effects by incorporating the fully spin-dependent code POLRAD [17] into our MC simulation. Figure 2 shows the total event distribution as a function of invariant mass in comparison with the MC simulation results obtained while using the cross section from the MAID model. The distribution was corrected for the background contribution due to cell events and for dead time. The target density was determined by normalizing the MC results to the data in the region of the elastic scattering peak as indicated by the open circles. The dotted and dot-dashed curves show the contributions from elastic and pion-production processes (including radiative effects). The inset of Fig. 2 shows the cross section extracted from our measured rates after subtracting the elastic scattering tail and correcting for radiative effects. The shaded area represents the size of the systematic uncertainty. The results are consistent with the cross section of the MAID model (solid curve) and the SL model (dashed curve). We averaged the model cross sections with our MC code over the Q^2 acceptance of the experiment for each W bin. The top scale of the inset indicates the average Q^2 for each W bin.

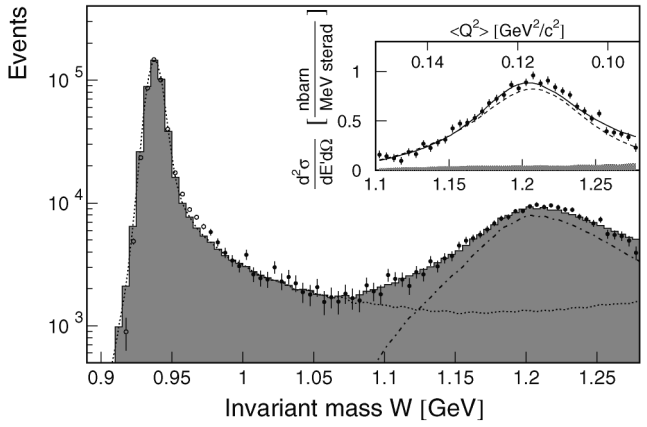

FIG. 2. Total event distribution as a function of W after background subtraction. The shaded histogram shows the MC results obtained with the MAID model cross section [16]. The dotted and dot-dashed curves show the contributions (with radiative effects) of elastic and pion-production processes. The data used for normalizing the luminosity are shown with open circles. Top-right inset: nonradiated cross section in the resonance region extracted from the data and compared with the prediction of the MAID (solid curve) and SL models (dashed curve) [7]. The shaded band shows the systematic uncertainty.

Provided the beam and target polarization product P_eP_p is known, the physics asymmetry A can be determined from an experimental asymmetry defined as $A_{\rm exp} \equiv (n_+ - n_-)/(n_+ + n_-) = P_eP_pA$, where $n_\pm$ are the numbers of events that pass the selection criteria, with either positive or negative polarization product, and normalized to the integrated luminosity for that state. Here, the rates $n_\pm$ are corrected for the background contribution due to cell events and for dead time. In our experiment, we determine the polarization product by normalizing the elastic scattering asymmetry to the predicted value. This asymmetry can be accurately calculated from the well-known elastic electron-proton scattering form factors (see, e.g., Ref. [3]). In this way, we determined $P_eP_p = 0.191 \pm 0.007$ (0.131 ± 0.013) for the parallel (perpendicular) spin orientation. The given uncertainties are dominated by the statistical accuracy. Note that, due to the large acceptance of the electron spectrometer, elastic scattering events were measured simultaneously to pion-production events.

Figure 3 shows our results for the $A_{\|\mathbf{q}_\Delta}$ and $A_{\perp\mathbf{q}_\Delta}$ spin correlation parameters as a function of the invariant mass W. The asymmetry data were normalized to the predicted value in the region $925 < W < 975$ MeV (open circles in Fig. 3). The (asymmetric) systematic errors $\delta_{\rm sys}$, indicated by the shaded area in the graph, include uncertainties originating from the cell wall background and cosmic event rates. The dominant error contribution is the one due to the cell wall background, the rate of which is approximately constant when plotted as a function of invariant mass W. As a consequence, $\delta_{\rm sys}$ is (approximately) proportional to the measured asymmetry and inversely

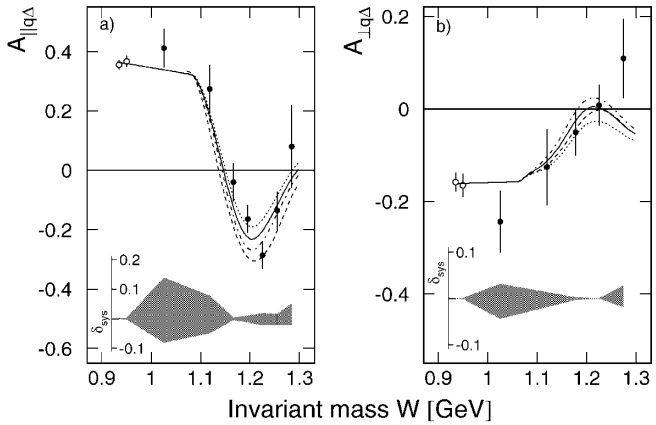

FIG. 3. Spin correlation parameters $A_{\|\mathbf{q}_\Delta}$ (left) and $A_{\perp\mathbf{q}_\Delta}$ (right) as a function of invariant mass W for inclusive ep scattering. The curves show predictions for the MAID and SL models (see text).

proportional to the signal-to-background ratio. Note that since the elastic scattering radiative tail contributes about 15% to the rates in the resonance region and since the elastic scattering asymmetry is sizable in these kinematics, a *spin-dependent* treatment of radiative effects is essential for comparing the measured asymmetries to model predictions. In Fig. 3, we compare our results to the MAID and SL model predictions. These were folded over the detector acceptance with our MC code, while radiative effects were taken into account with POLRAD. Both models describe reasonably well the global behavior of our spin correlation data. In particular, the data suggest steep slopes at the sides of the resonance region, where nonresonant processes are expected to dominate. These slopes are well reproduced by the models.

The agreement between the models and our data may be improved by adjusting the quadrupole strengths, which are relatively unconstrained model parameters. This is shown in the graphs of Fig. 3, where we plotted the MAID model predictions for different values of the $R_{EM} \equiv \mathrm{Re}\{M_{1+}^{3/2*} E_{1+}^{3/2}\}/|M_{1+}^{3/2}|^2$ and $R_{CM} \equiv \mathrm{Re}\{M_{1+}^{3/2*} S_{1+}^{3/2}\}/|M_{1+}^{3/2}|^2$ (at $W = 1232$ MeV). The dotted, solid, and dot-dashed curves show the predicted spin correlation parameters for $R_{EM} = +2.2\%$, -0.1%, and -2.2%, and for $R_{CM} = 0$, -7.9%, and -13% and give a measure of the sensitivity to and linear dependence of $A_{\parallel \mathbf{q}_\Delta}$ ($A_{\perp \mathbf{q}_\Delta}$) on the parameter R_{EM} (R_{CM}). The dashed curves show the predictions of the SL model with an R_{EM} (R_{CM}) of -2% (-4.2%). The default values of MAID at $Q^2 = 0.11$ GeV$^2/c^2$ were $R_{EM} = -2.2\%$ and $R_{CM} = -6.5\%$. We varied these independently by multiplying the corresponding quadrupole resonance couplings by a factor (while keeping the same dipole resonance coupling) and calculating a χ^2 from the comparison of the predicted spin correlation parameters to our $A_{\parallel \mathbf{q}_\Delta}$ and $A_{\perp \mathbf{q}_\Delta}$ data in the range $1160 < W < 1275$ MeV. Minimum χ^2 were obtained for $R_{EM} = -0.1\% \pm 1.7\%(\mathrm{stat})^{+1.0}_{-0.9}\% \times (\mathrm{syst})$ ($\chi^2_{\mathrm{min}}/N_{\mathrm{DF}} = 0.85$) and $R_{CM} = -7.9\% \pm 9.1\% \times (\mathrm{stat})^{+0.4}_{-0.5}\%(\mathrm{syst})$ ($\chi^2_{\mathrm{min}}/N_{\mathrm{DF}} = 1.02$). Here, N_{DF} is the number of degrees of freedom in the χ^2 minimization. As for the spin correlation data, the quoted systematic errors for the R_{EM} and R_{CM} are dominated by the uncertainties stemming from the cell background contribution, but include as well the contributions from the normalization of the polarization product and the magnetic field angles.

In summary, we have presented cross sections and first data on the spin correlation parameters $A_{TT'}$ and $A_{TL'}$ in the invariant mass range covering the Δ resonance region in inclusive electron-proton scattering. These data provide a stringent test for model predictions of polarization observables in electroproduction of pions. We compared our results to the theoretical models of Drechsel *et al.* (MAID) and Sato and Lee. Both give a reasonable description of our data over the entire Δ resonance region.

We are grateful to the NIKHEF and VU technical groups for their outstanding support. We thank T. Sato, T.-S. H. Lee, and the MAID group for making their calculations available to us. This work was supported in part by the Stichting voor Fundamenteel Onderzoek der Materie (FOM), which is financially supported by the Nederlandse Organisatie voor Wetenschappelijk Onderzoek (NWO), the National Science Foundation under Grant No. HRD-9633750 (Hampton University) and the Swiss National Foundation.

[1] F. Kalleicher *et al.,* Z. Phys. A **359**, 201 (1997); V. V. Frolov *et al.,* Phys. Rev. Lett. **82**, 45 (1999); C. Mertz *et al., ibid.* **86**, 2963 (2001); Th. Pospischil *et al., ibid.* **86**, 2959 (2001); K. Joo *et al., ibid.* **88**, 122001 (2002).

[2] R. Beck *et al.,* Phys. Rev. Lett. **78**, 606 (1997); G. Blanpied *et al., ibid.* **79**, 4337 (1997); R. Beck *et al.,* Phys. Rev. C **61**, 035204 (2000); G. Blanpied *et al., ibid.* **64**, 025203 (2001).

[3] T. W. Donnelly and A. S. Raskin, Ann. Phys. (N.Y.) **169**, 247 (1986); A. S. Raskin and T. W. Donnelly, *ibid.* **191**, 78 (1989).

[4] D. Drechsel and L. Tiator, J. Phys. G **18**, 449 (1992).

[5] I. G. Aznauryan, Phys. Rev. D **57**, 2727 (1998).

[6] S. S. Kamalov and Shin Nan Yang, Phys. Rev. Lett. **83**, 4494 (1999).

[7] T. Sato and T.-S. H. Lee, Phys. Rev. C **63**, 055201 (2001); **54**, 2660 (1996).

[8] Y. B. Dong, K. Shimizu, and A. Faessler, Nucl. Phys. **A689**, A889 (2001); M. Fiolhais, B. Golli, and S. Širca, Phys. Lett. B **373**, 229 (1996).

[9] A. J. Buchmann, E. Hernández, U. Meyer, and A. Faessler, Phys. Rev. C **58**, 2478 (1998).

[10] A. J. Buchmann, E. Hernández, and A. Faessler, Phys. Rev. C **55**, 448 (1997).

[11] D. Szczerba *et al.,* Nucl. Instrum. Methods Phys. Res., Sect. A **455**, 769 (2000); L. D. van Buuren *et al., ibid.* **474**, 209 (2001).

[12] H. R. Poolman *et al.,* Phys. Rev. Lett. **84**, 3855 (2000).

[13] B. Militsyn, Ph.D. thesis, Technical University of Eindhoven, 1998.

[14] I. Passchier *et al.,* Nucl. Instrum. Methods Phys. Res., Sect. A **414**, 446 (1998).

[15] D. J. J. de Lange *et al.,* Nucl. Instrum. Methods Phys. Res., Sect. A **412**, 254 (1998); **406**, 182 (1998).

[16] D. Drechsel, O. Hanstein, S. S. Kamalov, and L. Tiator, Nucl. Phys. **A645**, 145 (1999); we used the "standard" MAID2000 version, see http://www.kph.uni-mainz.de/MAID/maid2000/.

[17] I. V. Akushevich and N. M. Shumeiko, J. Phys. G **20**, 513 (1994).